

Comparison between TiO₂/rGO and TiO₂ with Various Microelectrode Gaps for Biosensor Applications

Roharsyafinaz Roslan^a, Noraziah Mohamad Zin^b, Anis Amirah Alim^a, Sharipah Nadzirah^a, Nurkhaizan Zulkepli^a, Chang Fu Dee^a, P Sushthitha Menon^a, Ahmad Ghadafi Ismail^a and Azrul Azlan Hamzah^{a*}

^aInstitute of Microengineering and Nanoelectronics, National University of Malaysia (UKM), 43600 Bangi, Selangor.

^bUKM Medical Biology Institute, National University of Malaysia (UKM), 43600 Bangi, Selangor.

*Corresponding author. Tel.: +6019-3393429; e-mail: azlanhamzah@ukm.edu.my

ABSTRACT

Sensitive, selective, and stable materials are important to act as an electron transport layer to construct signals in biosensors. Graphene-based biosensors get attention in this industry due to their selective and sensitive properties. We fabricated TiO₂/rGO and TiO₂ using spin coating in this study. Thermal evaporation deposited the silver. The picoammeter examined the influence of microelectrode gap sizes (50, 100, and 250 μm) on electrical performance. It was revealed that a smaller gap generates better electrical performance. At the smallest gap, the 50 μm TiO₂ (8.04E-12 A) and TiO₂/rGO (2.385E-8 A) at 0.04V. The morphological and chemical analysis supported the electrical behavior of TiO₂/rGO and TiO₂. These results show that the method used was able to form a TiO₂/rGO film that is sensitive to the size of the gap between two microelectrodes.

Keywords: Source-drain Gap, Sol-gel method, TiO₂, TiO₂-rGO

1. INTRODUCTION

A biosensor is an analytical device that detects the presence of a chemical compound by utilising a biological component with a physicochemical detector. Since the 1960s, many sensors for biosamples have been discovered. For example, piezoelectric biosensors [1], [2] enzyme-based biosensors [3], and deoxyribonucleic acid (DNA) biosensors [4]. A transducer, such as an electrical signal [5], translates the response from a biological sample into a measurable signal [5]. The choice of transducer for each sensor depends on the mechanism by which the sensors work. Generally, transducer materials are classified as conductors, insulators, or semiconductors [2]. Metal oxide semiconductors, such as titanium dioxide (TiO₂), tin oxide (SnO₂), and zinc oxide (ZnO), are commonly used due to their large surface area, biocompatibility, high stability, and low cost. The biosensors industry widely employs metal oxide semiconductors [3]–[5]. One of the materials used in this research is titanium dioxide, as a highlight.

TiO₂ is a non-toxic material with uncommon chemical and physical properties. Typically, TiO₂ is an n-type semiconductor with an optical band gap of 3.2 eV. Because of its comparatively good performance and stability, TiO₂ is commonly used in the fabrication of electronic and optoelectronic devices, for example, photodetectors [6], and dye-sensitised solar cells (DSSCs) [7]. A few studies show that TiO₂-based sensors have high selectivity and sensitivity for detecting biomolecules such as glucose [8].

Other than semiconductors, graphene is also a common material in the electrical industry. Graphene is a single layer of carbon atoms tightly arranged in a honeycomb

configuration and exhibiting high charge carrier mobility, high conductivity, and mechanical strength. It can be synthesised in several methods such as mechanical exfoliation [9], epitaxial growth [10], ion-beam irradiation [11], and chemical vapour deposition (CVD). It is the most favourable transducer material for use in sensors [3]. However, the absence of defects in pure graphene leads to difficulties in functionalization. Other derivatives of graphene, such as graphene oxide (GO) and reduced graphene oxide (rGO), have the potential for bioreceptor immobilisation due to the abundance of functional groups in their structures [12].

At the moment, there is a lot of excitement in the industry about carbon-based sensors, such as GO-based sensors [13]. Due to its unique properties, 2D material has high electron mobility, high electrical conductivity, and high thermal conductivity. This is because oxygenated functional groups pass through the edges and planes of the layered sp³ carbon atoms [14]. The GO-based biosensor served as a flexible biosensor for wearable devices. Chemically oxidizing graphene to form graphene oxide led to the discovery of improvements in graphene as an electron transport layer (ETL) [15]. It shows better physical and electrical properties or carbon-based biosensors [12].

Modification of transducer material revealed an improvement in the selectivity and sensitivity of biosensors rather than single-material transducers. As an illustration, previous research revealed that both TiO₂-graphene biosensors and TiO₂ biosensors can detect glucose at 6.2 mM and 6.7 mM [8], [16] This is due to the combination of unique properties of TiO₂ and graphene

that is able to enhance the synergistic effect between glucose and the transducer [16]. Furthermore, the composition of TiO₂ and graphene creates a wider surface-to-volume ratio that facilitate electron transfer between biosample and electrode through electron injection to graphene from the TiO₂ conduction band [17], [18]. Every modified or composite material has an attractive property.

We investigated the effect of fabricating two microelectrodes on TiO₂ and TiO₂/rGO with different gap sizes (50, 100, and 250 μm). We also report on the performance of both materials which, have excellent electrical properties.

2. THEORETICAL BACKGROUND

The working principle of biosensors is most likely similar to that of a metal oxide field effect transistor (MOSFET). The fabrication of FET commonly involves photolithography, etching, [19], [20] and metallization. The transducer material in the channel region acts as a connection, converting the external charge of biomolecule interaction. Previous work [21], has explained further information on the theoretical algorithm.

3. METHODOLOGY

3.1. Synthesis of TiO₂/rGO Thin Film

There are a few methods used to synthesise TiO₂ solutions, such as the hydrothermal method, the sol-gel method, and wet-chemical synthesising by precipitation of hydroxides from salts [6], [22]. In this research, titanium dioxide (TiO₂) and titanium dioxide/graphene oxide (TiO₂/GO) were prepared using the sol-gel method as referred to in previous research [4]. A titanium precursor solution of Titanium Isopropoxide (TTIP), ethanol, and acetic acid was stirred for two hours at 80 °C (TTIP: acetic acid : ethanol 1:0.02:9 ratio). A GO solution was prepared by dispersing 40 mg of GO powder into 10 ml of ethanol. The solution was then ultrasonicated for 1 hour and was well dispersed in the solution. 0.1% of the GO solution was mixed in the TiO₂ solution for 1 hour at 80 °C and rested at room temperature for a minimum of 8 hours before the spin coat. The obtained TiO₂/rGO was spin-coated on a Si/SiO₂ substrate and annealed in a tube furnace in the presence of H₂ and Ar gas at 600 °C for 1 hour to crystallise the titanium dioxide and reduce the graphene oxide.

3.2. Fabrication of Electrodes

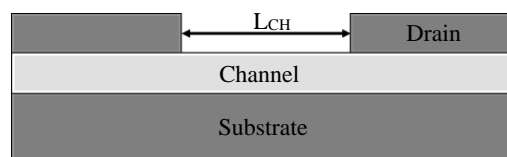


Figure 1. Illustration of fabricated microelectrode devices with various gap sizes.

The conventional photolithography process can produce stable and low contact resistances [23]. However, the use of chemicals during metallization or lift-off could compromise the unique properties of the materials. To overcome the limitations of the above techniques, the best approach to producing low resistance and stable electrical contacts is by using a shadow mask. A shadow mask is a precision, micromachined sheet or metal plate that is used in various metal deposition processes.

Si/SiO₂ substrate is used. Different microelectrode gaps (L_{CH}) of 250 μm, 100 μm, and 50 μm were fabricated on the TiO₂ and TiO₂/rGO samples. Excellent uniformity of spin-coated TiO₂/rGO and TiO₂ was observed throughout the sample using Raman spectroscopy and FE-SEM. 80 nm-thick silver electrode was deposited on the sample using a stainless steel shadow mask, as shown in Figure 1 by thermal evaporation at a rate of 0.5 Å/s at 1.8 V and 1.1 Å/s at 1.3 V.

4. DATA COLLECTION AND ANALYSIS

4.1. Chemical Analysis by Raman Spectroscopy

Raman spectroscopy is a technique for non-destructive chemical examination that provides extensive information about chemical structure, phase and polymorphy, crystallinity, and molecular interactions. It is based on light's interaction with vibrated chemical bonds within a substance.

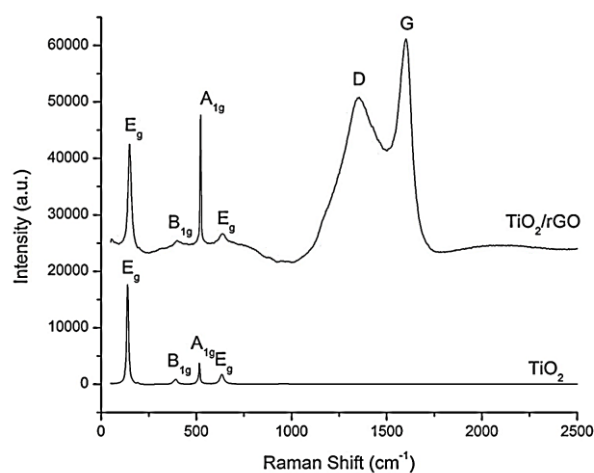


Figure 2. Raman spectroscopy analysis for TiO₂/rGO and TiO₂ thin film.

TiO₂ and TiO₂/rGO thin films were characterised by their Raman spectra, Figure 2, which allow for consideration of the conjugated, and carbon-carbon double bonds, which lead to high-intensity peaks in the Raman spectrum. The four typical Raman spectra of characteristic active modes of anatase TiO₂ with symmetries E_g, B_{1g}, A_{1g}, and E_g were observed at 144, 400, 519, and 640 cm⁻¹ and peaks B_{1g}, E_g, and A_{1g} for 140, 430, and 590 cm⁻¹, respectively, in rutile TiO₂. [24], [25] Figure 2 reveals the peaks of E_g, B_{1g}, A_{1g}, and E_g at 139.06, 391.69, 515.12, and 632.76 cm⁻¹. These characteristics of vibrational frequencies and their intensity ratios confirmed the phase of pure anatase TiO₂. The peaks revealed by TiO₂/rGO area at 148.7, 397.48, 522.83, and 636.61 cm⁻¹, respectively. Moreover, the raman of TiO₂/rGO shows the D band peak at 1348.12 cm⁻¹, which is a characteristic peak that indicates the presence of defects, particularly in carbon-based materials like reduced graphene oxide.

4.2. Morphological Analysis by FESEM

Figure 3 displays an image of the surface morphology of TiO₂ and TiO₂/rGO thin films. The TiO₂ forms in anatase appear to consist of a few fused spheres, while TiO₂/rGO form imperfectly merged spherical shapes [26]. The surface of TiO₂/rGO was found to be relatively smoother when compared to anatase. This morphology is consistent with recent findings from previous investigations [22].

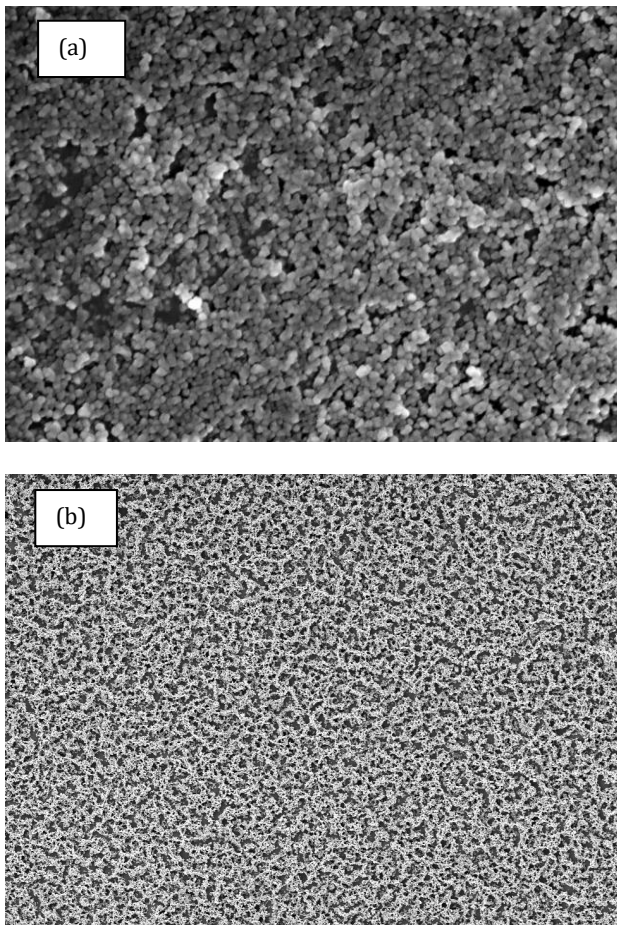
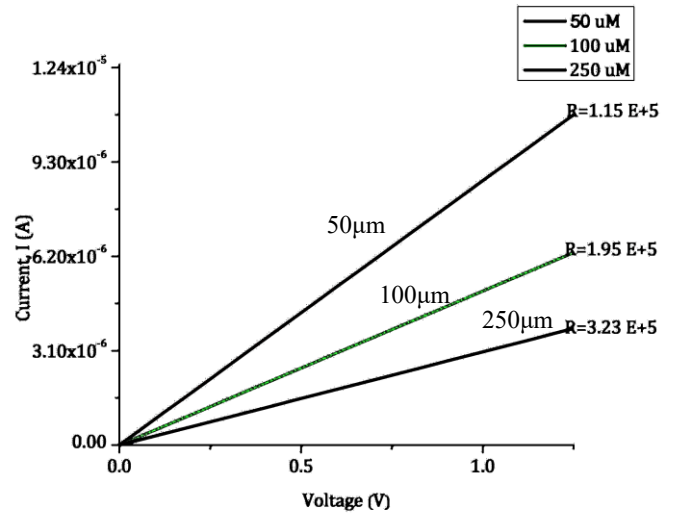


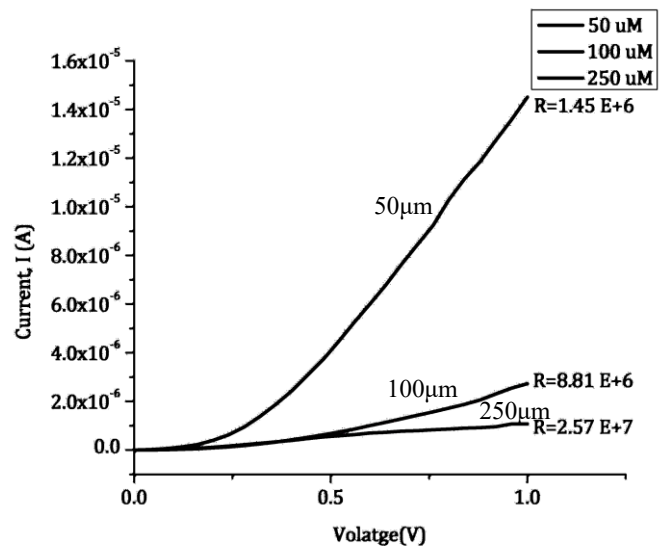
Figure 3. Morphological result of (a)TiO₂ and (b)TiO₂/rGO thin film on Si/SiO₂ substrates.

4.3. Electrical Characterization by Picoammeter

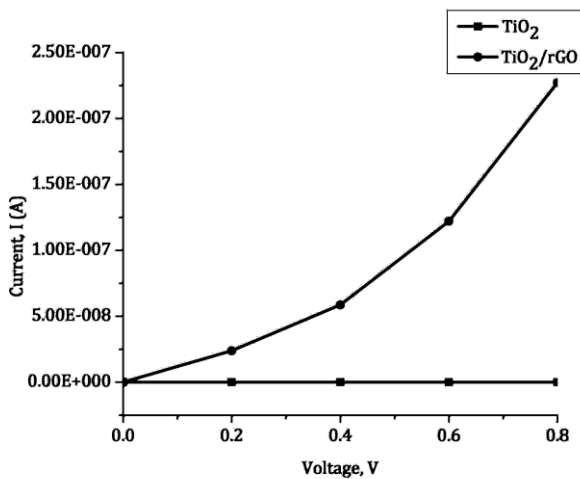
Figure 4 shows the current-voltage (I-V) measurement of the devices. The current output and resistance inside the channel were investigated using SMU instruments in DC mode with channel variations of 250 μm, 100 μm, and 50 μm. Both materials show that the smaller the microelectrode gaps, the lower the resistance of the channel, which results in less voltage drop across it for a given current.



(a)



(b)



(c)

Figure 4. I-V graph of (a) TiO₂ and (b) TiO₂/rGO with different sizes of source-drain gap and (c) current generated by TiO₂ and TiO₂/rGO at 0-0.8V.

5. RESULTS AND DISCUSSION

Chemical properties affect the conductivity of materials [25]. As referred to in Figure 2, the peaks show anatase TiO₂ vibrational modes, while in TiO₂/rGO, they represent the peaks of TiO₂ anatase but are shifted to the left. That may be caused by the presence of rGO, which affects the structural and vibrational frequencies. The D band in TiO₂/rGO represents the defects in the graphene material. It shows the graphene form is imperfect and may contain dangling function groups such as carbonyl, epoxy, and hydroxyl. The presence of reduced graphene oxide, may lead to a high surface area for the sample to attach and transfer signals [5].

Moreover, the structure of materials affects their electrical properties. As shown in Figure 4(C), TiO₂/rGO has better electron transport properties than TiO₂ compared with TiO₂ [27]. It may be caused by the addition of rGO, which provides more carbon bonding and a wider area of rGO nanosheets. But, the surface area and effectiveness as electron transport layers for both materials, TiO₂ and TiO₂/rGO make them suitable to act as transducers in biosensors.

In addition, there are a few parameters that have an impact on biosensor effectiveness [5]. For example, the size of the channel, the width of the electrode, the thickness of the electrode, and the thickness of the transducer [12]. The size of the microelectrode gap has the highest impact on the sensitivity of the sensor, with a wider gap between two microelectrodes, resistance increased, as shown in figures 4 (a) and (b). This study shows that TiO₂ and TiO₂/rGO are able to produce better current in the microampere range with a 50 μ m gap and minimum voltage applied. In future studies, we expect that TiO₂ and TiO₂/rGO will be able to detect the small amount of biosamples with a low limit of detection.

Currently, the biosensor industry has focused on miniaturisation due to the possibility of achieving lower detection limits from micromolar to femtomolar. Previous studies prove that the most suitable output current for biosensor applications is in the range of microns and nanoamperes [28]. The simulation study in previous work has shown that the TiO₂/rGO material increases its current performance by reducing the gap of the channel [21]. In this study, we have proved experimentally that TiO₂ and TiO₂/rGO could conduct in smaller channel lengths with current output in the range of microns.

6. CONCLUSION

We have developed microelectrodes using TiO₂ and TiO₂/rGO sol-gel spin-coating techniques. Raman spectroscopy and FESEM analysis have proven the presence and quality of both materials. I-V measurement shows that the microelectrode with the smallest gap size has the highest output current response for TiO₂ (8.04E-12 A) and TiO₂/rGO (2.385E-8 A) at 0.04V. In terms of electrical characterization, the two electrodes show that TiO₂/rGO has better conductivity than TiO₂. It is due to the presence of rGO. However, both materials show a good potential interface contact that can act as a great transducer material for biosensor applications. The straight-forward steps of synthesis material presented in this work will facilitate the fabrication of biosensor devices in the future while at the same time lowering the cost of manufacturing and preventing thermal denaturation of bio-samples.

ACKNOWLEDGMENTS

The authors would like to express their gratitude to the National University of Malaysia (UKM) for sponsoring this study through the translation research grant (UKM-TR) under grant number UKM-TR-014. The characterizations were done together with i-CRIM laboratory, National University Malaysia. The author would also like to thank all of the team members from the Institute of Microengineering and Nanoelectronics (IMEN), National University of Malaysia (UKM), for their advice and assistance.

REFERENCES

- [1] A. A. Hamzah, B. Y. Majlis, and I. Ahmad, "Deflection analysis of epitaxially deposited polysilicon encapsulation for MEMS devices," *Proc. ICSE 2004 - 2004 IEEE Int. Conf. Semicond. Electron.*, vol. 00, no. c, pp. 611-614, 2004, doi: 10.1109/smelec.2004.1620960.
- [2] N. Marsi, B. Y. Majlis, A. A. Hamzah, and F. Mohd-Yasin, "Comparison of mechanical deflection and maximum stress of 3C SiC- and si-based pressure sensor diaphragms for extreme environment," *2012 10th IEEE Int. Conf. Semicond. Electron. ICSE 2012 - Proc.*, pp. 186-190, 2012, doi:

- 10.1109/SMElec.2012.6417120.
- [3] X. Liu *et al.*, "Enzyme-coated single ZnO nanowire FET biosensor for detection of uric acid," *Sensors Actuators, B Chem.*, vol. 176, no. 2010, pp. 22–27, 2013, doi: 10.1016/j.snb.2012.08.043.
- [4] S. Nadzirah *et al.*, "State-of-the-Art on Functional Titanium Dioxide-Integrated Nano-Hybrids in Electrical Biosensors," *Crit. Rev. Anal. Chem.*, vol. 52, no. 3, pp. 637–648, 2022, doi: 10.1080/10408347.2020.1816447.
- [5] N. Bhalla, P. Jolly, N. Formisano, and P. Estrela, "Introduction to biosensors," *Essays Biochem.*, vol. 60, no. 1, pp. 1–8, 2016, doi: 10.1042/EBC20150001.
- [6] Y. Gao *et al.*, "TiO₂ Nanorod Arrays Based Self-Powered UV Photodetector: Heterojunction with NiO Nanoflakes and Enhanced UV Photoresponse," *ACS Appl. Mater. Interfaces*, vol. 10, no. 13, pp. 11269–11279, 2018, doi: 10.1021/acsami.7b18815.
- [7] R. Kemat, S. K. Sahari, and A. Baharin, "The effects of annealing temperature dependence on the doping of titanium dioxide (TiO₂) and reduced graphene oxide (RGO) for perovskite solar cell application," *Int. J. Nanoelectron. Mater.*, vol. 13, no. 3, pp. 421–432, 2020.
- [8] B. Gopal Krishna, M. J. Rao, B. Nalinikant, D. K. Golhani, and S. Tiwari, "Highly sensitive TiO₂ thin film matrix biosensor for glucose detection in blood," *IEEE Reg. 10 Annu. Int. Conf. Proceedings/TENCON*, no. 100, pp. 2947–2951, 2017, doi: 10.1109/TENCON.2016.7848585.
- [9] M. Yi and Z. Shen, "A review on mechanical exfoliation for the scalable production of graphene," *J. Mater. Chem. A*, vol. 3, no. 22, pp. 11700–11715, 2015, doi: 10.1039/c5ta00252d.
- [10] G. R. Yazdi, T. Iakimov, and R. Yakimova, "Epitaxial graphene on SiC: A review of growth and characterization," *Crystals*, vol. 6, no. 5, 2016, doi: 10.3390/cryst6050053.
- [11] A. V. Krashennnikov and K. Nordlund, "Ion and electron irradiation-induced effects in nanostructured materials," *J. Appl. Phys.*, vol. 107, no. 7, 2010, doi: 10.1063/1.3318261.
- [12] W. K. Pang, K. L. Foo, S. J. Tan, S. C. B. Gopinath, and C. H. Voon, "Study on graphene oxide and reduced graphene oxide overlaid on field effect transistor with channel length variation," *2019 IEEE Int. Conf. Sensors Nanotechnology, SENSORS NANO 2019*, pp. 1–4, 2019, doi: 10.1109/SENSORSNANO44414.2019.8940061.
- [13] Y. Sun and V. Kursun, "N-Type carbon-nanotube MOSFET device profile optimization for very large scale integration," *Trans. Electr. Electron. Mater.*, vol. 12, no. 2, pp. 43–50, 2011, doi: 10.4313/TEEM.2011.12.2.43.
- [14] Z. Zhen and H. Zhu, "Structure and Properties of Graphene," in *Graphene*, Elsevier, 2018, pp. 1–12.
- [15] I. Childres, L. A. Jauregui, W. Park, H. Caoa, and Y. P. Chena, "Raman spectroscopy of graphene and related materials," *New Dev. Phot. Mater. Res.*, pp. 403–418, 2013.
- [16] H. D. Jang, S. K. Kim, H. Chang, K. M. Roh, J. W. Choi, and J. Huang, "A glucose biosensor based on TiO₂-Graphene composite," *Biosens. Bioelectron.*, vol. 38, no. 1, pp. 184–188, 2012, doi: 10.1016/j.bios.2012.05.033.
- [17] H. Xu, H. Dai, and G. Chen, "Direct electrochemistry and electrocatalysis of hemoglobin protein entrapped in graphene and chitosan composite film," *Talanta*, 2010, doi: 10.1016/j.talanta.2009.12.006.
- [18] A. Azani *et al.*, "Recent graphene oxide/TiO₂ thin film based on self-cleaning application," *IOP Conf. Ser. Mater. Sci. Eng.*, vol. 572, no. 1, 2019, doi: 10.1088/1757-899X/572/1/012079.
- [19] A. A. Hamzah, J. Yunas, B. Y. Majlis, and I. Ahmad, "Sputtered encapsulation as wafer level packaging for isolatable MEMS devices: A technique demonstrated on a capacitive accelerometer," *Sensors*, vol. 8, no. 11, pp. 7438–7452, 2008, doi: 10.3390/s8117438.
- [20] A. A. Hamzah, B. Y. Majlis, and I. Ahmad, "HF Etching of Sacrificial Spin-on Glass in Straight and Junctioned Microchannels for MEMS Microstructure Release," *J. Electrochem. Soc.*, vol. 154, no. 8, p. D376, 2007, doi: 10.1149/1.2742302.
- [21] A. A. Alim *et al.*, "Geometrical Characterisation of TiO₂ -rGO Field-Effect Transistor as a Platform for Biosensing Applications," pp. 1–18, 2023.
- [22] R. K. Nainani *et al.*, "Sol-Gel Synthesis of Titanium Dioxide," *Crit. Rev. Anal. Chem.*, vol. 73, no. 3, pp. 20184–20196, 2022, doi: 10.1080/10408347.2020.1816447.
- [23] R. S. Selvarajan, B. Y. Majlis, M. A. Mohamed, and A. A. Hamzah, "Optimization of lift off process in electrode patterning for graphene based field effect transistor," *ASM Sci. J.*, vol. 12, no. SpecialIssue4, pp. 76–82, 2019.
- [24] S. Challagulla, K. Tarafder, R. Ganesan, and S. Roy, "Structure sensitive photocatalytic reduction of nitroarenes over TiO₂," *Sci. Rep.*, vol. 7, no. 1, pp. 1–11, 2017, doi: 10.1038/s41598-017-08599-2.
- [25] W. Su, J. Zhang, Z. Feng, T. Chen, P. Ying, and C. Li, "Surface phases of TiO₂ nanoparticles studied by UV raman spectroscopy and FT-IR spectroscopy," *J. Phys. Chem. C*, vol. 112, no. 20, pp. 7710–7716, 2008, doi: 10.1021/jp7118422.
- [26] A. S. Bakri *et al.*, "Effect of annealing temperature of titanium dioxide thin films on structural and electrical properties," *AIP Conf. Proc.*, vol. 1788, 2017, doi: 10.1063/1.4968283.
- [27] S. Nadzirah, U. Hashim, M. R. Zakaria, and M. Rusop, "Electrical properties of titanium dioxide nanoparticle on microelectrode: Gap size effect," *AIP Conf. Proc.*, vol. 1963, pp. 1–6, 2018, doi: 10.1063/1.5036919.
- [28] A. Wasfi, F. Awwad, J. G. Gelovani, N. Qamhieh, and A. I. Ayesh, "COVID-19 Detection via Silicon Nanowire Field-Effect Transistor: Setup and Modeling of Its Function," *Nanomaterials*, vol. 12, no. 15, 2022, doi: 10.3390/nano12152638.